J5.4 3D AIR QUALITY AND THE CLEAN AIR INTERSTATE RULE: LAGRANGIAN SAMPLING OF CMAQ MODEL RESULTS TO AID REGIONAL POLLUTION ACCOUNTABILITY METRICS

T. Duncan Fairlie[1*], James Szykman[2], R. Bradley Pierce[3], Alice Gilliland[3]
Jill Engel-Cox[4], Stephanie Weber[4], Chieko Kittaka[5], J. Al-Saadi[1],
Rich Scheffe[2], Fred Dimmick[2], Joe Tikvart[2]

[1] NASA; [2] U.S. EPA; [3] NOAA
[4] Battelle Memorial Institute, [5]SSAI

1. Introduction

*The U.S. EPA **Clean Air Interstate Rule** (CAIR) is expected to reduce regional transport of fine sulfate particles in non-attainment areas in Eastern. U.S. An integrated air quality observational and modeling system is needed to understand regional transport contributions, and monitor impact of CAIR reductions. The goal of this study is to demonstrate how a 3-d monitoring network of ground-based and satellite observations can be integrated with results from a 3-d regional air quality model and a Lagrangian trajectory model to enhance understanding of particulate pollution transport, and improve pollution source attribution, to aid in developing regulatory "air-transport-related" accountability metrics for a principal East Coast metropolitan area. We use ensemble-mean back trajectory sampling of EPA's Community Multi-scale Air Quality (CMAQ) model (CMAQ) results to characterize key sources of sulfate pollution, and chemical/physical histories of air arriving in the daytime boundary layer at Baltimore, MD. We integrate NASA satellite (MODIS) and AirNOW surface data with model results, and estimate the relative contributions of regional transport vs. local sources to fine particle air pollution events at Baltimore. Initial results of this work are reported by Weber et al. [Clean Air Interstate Rule (CAIR) Accountability Assessment: An Integrated Model-Measurement Approach to Assess Synoptic-Scale Transport of Sulfate Aerosols, U.S. Environmental Protection Agency Advanced Monitoring Initiative Report, 2008].

2. **Data and Model descriptions**

PM2.5 data shown here are taken from the continuous Tapered Element Oscillating Microbalance (TEOM) analyzer at Old Town, Baltimore. Sulfate data are taken from the monitors at the IMPROVE site at Baltimore, and the Speciated Trends Network (STN) sites at Fort Meade, and Essex, MD. Aerosol Optical Depth data shown here are taken from the Moderate Resolution Imaging Spectroradiometer (MODIS) sensor on the Terra satellite, and from the AERONET instrument at the MD Science Center.

Simulated aerosol and gas phase concentrations used in this study are taken from a 3-month simulation for summer 2004 conducted with the U.S. EPA's Models 3/Community Multi-scale Air Quality (CMAQ) modeling system, version 4.5 (Byun and Schere, 2006; Byun and Ching, 1999). The CMAQ version used here uses the Carbon Bond IV chemical mechanism (Gery *et al.*, 1989), with aerosol predictions based on a modal aerosol model (Binkowski and Roselle, 2003) and the ISORROPIA thermodynamic equilibrium model (Nenes *et al.*, 1998). The emissions inventory used was the National Emissions Inventory (NEI) for 2001. Continuous Emissions Monitoring System (CEMS) data for 2004 were used for power plants. Mobile source estimates were attained using the EPA's MOBILE6 vehicle emissions model with 2004 fleet and driving information. The summer 2004 simulation was conducted using a rectangular domain covering the Eastern United States and southeastern Canada. The simulation used a 12 km horizontal grid resolution, and 14 sigma levels in the vertical extending from the ground to the tropopause. The CMAQ domain and horizontal grid is shown in Fig.1. The CMAQ simulation was driven by Meteorology Chemistry Interface Processor (MCIP) fields predicted by a succession of 5-day simulations for June through August 2004 with the non-hydrostatic Mesoscale Meteorology model (MM5). A 10-day spin-up of CMAQ was conducted prior to 1 June. The CMAQ simulation was conducted with "clean" boundary conditions, i.e. concentration estimates being transported in from lateral

* *Corresponding author address*: T. Duncan Fairlie, NASA Langley Research Center, Hampton, VA-23681, USA; email: t.d.fairlie@nasa.gov

boundaries are simple average estimates based on observational data in non-polluted areas. Consequently, episodic sources of carbonaceous aerosol external to the domain, e.g. Alaskan wildfires in summer 2004 (Pfister et al., 2005; Clarke et al., 2007), are not represented. Transport of sulfate from outside the domain is considered small.

CMAQ and MCIP products are made available at 1-hr intervals from 1 June to 31 August, 2004. CMAQ products used in this study include aerosol sulfate, nitrate, ammonium, organic and elemental carbon components, and gas phase sulfur dioxide, sulfuric acid, and ammonia. MCIP products include horizontal and vertical wind components, temperature, specific humidity, cloud and rainwater content. Derived products include fine particle ($PM_{2.5}$) concentrations, obtained from summing aerosol Aitken and accumulation (fine) components, and reconstructed aerosol extinction. The latter is estimated from the fine aerosol concentrations and relative humidity (RH):

$$B_{ext} = 3\, f(RH)\, ([NH_4^+] + [SO_4^=] + [NO_3^-]) + 4\, [OM] + 10\, [EC] + 1\, [FS] \quad \text{(Equ. 1)}$$

(Malm *et al*., 2004), where brackets indicate aerosol mass concentration in μg m^{-3}; abbreviations OM, FS, and EC represent Organic Mass, Fine Soil, and Light Absorbing Carbon, respectively. The coarse mass contribution to the aerosol extinction, 0.6 [CM], is not included, following Binkowski and Roselle (2003). The specific scattering and absorption coefficients (3, 4, 10, and 1) in the expression above have units $m^2\ g^{-1}$, the aerosol growth factor, f(RH), a function of relative humidity derived from MCIP fields, is obtained from a lookup table (Binkowski and Roselle, 2003; Malm *et al*., 1994). Aerosol extinction (B_{ext}) is expressed in Mm^{-1}. Aerosol optical depth (AOD) is obtained by integrating Bext over the vertical domain of the model, following the approach of Roy *et al.* (2007).

2.3 NASA Langley Trajectory Model

A Lagrangian trajectory model provides a low cost alternative to the emissions separation [Tao et al., 2003] or tagged tracer [Fast et al., 2002] techniques, commonly used in Eulerian models for source-receptor and apportionment studies. Here, we use a hybrid approach in which Lagrangian trajectories are used to sample 3-d Eulerian fields from the CMAQ model. We use the NASA Langley Trajectory Model (LaTM)

(Pierce and Fairlie, 1993; Pierce *et al.,* 1994) to estimate the source/receptor relationships for air masses transported into the Baltimore region. The LaTM is configured to use the same MCIP 3-D meteorological fields that drive CMAQ. 3-d ensemble-mean back trajectories (longitude, latitude, pressure) are computed using the horizontal and vertical components of the MCIP wind fields.

The LaTM is used to sample CMAQ aerosol, gas-phase, and MCIP meteorological fields along 3-day ensemble-mean back trajectories, originating in the Baltimore MSA. Lagrangian mean and variances of trajectory-sampled components are then computed. The Lagrangian samplings provide estimates of the mean and variance of air mass histories for air reaching the daytime boundary layer (BL) over the Baltimore area; these histories reflect the impact of source emissions, chemical transformations, deposition losses, and turbulent convective mixing. In particular, the Lagrangian samplings of CMAQ sulfate, and $PM_{2.5}$ provide estimates of the regional transport and local contributions to particulate levels in the Baltimore area for summer 2004.

A subtlety of our approach concerns the representation of sub-grid-scale processes such as turbulent convection and diffusion. LaTM trajectories are driven by winds represented explicitly on the MCIP grid, and do not experience sub-grid-scale turbulent motions directly. Instead, sub-grid-scale turbulent processes are represented via the CMAQ fields sampled by the LaTM, which *have* been exposed to such processes. This approach differs from alternative approaches, which include parameterized convective and turbulent dispersion in the trajectory calculations (Stohl et al., 1998). By accounting for Lagrangian mean influences of mixing on parcel chemical and physical properties we allow parcel identities to change, rather than maintain parcel identity but allow sub-grid-scale processes to impact position.

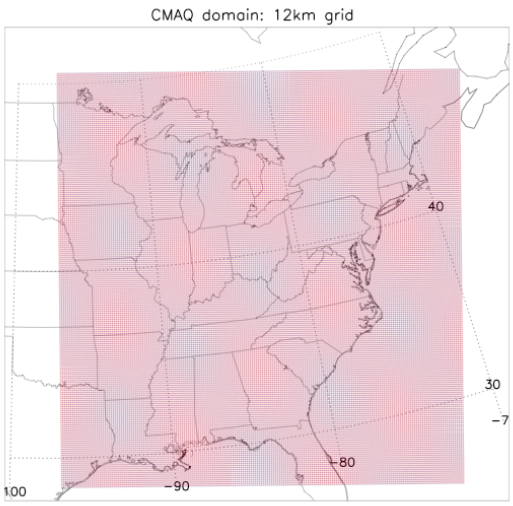

Figure1. CMAQ domain and grid.

Back trajectories are calculated for each day during the 3-month period from June to August. Trajectory clusters (or ensembles) are initialized at 18Z (2 pm EDT) each day at multiple levels - 20, 100, 500, 1000 m above ground level - centered at Baltimore. The trajectories are initialized at 2 pm local time to place them squarely within the boundary layer, which generally reaches its maximum depth in early to mid afternoon at this time of year. Trajectory ensembles initialized at multiple levels permit dispersion due to vertical shear in the winds, and provide an estimate of spatial variability in the origin of air arriving in the BL over Baltimore. [N.B., trajectories initialized at specific altitudes over Baltimore are subject to the full 3-D MCIP winds and do not remain at those altitudes.] In some cases, back trajectory calculations indicate that air arriving in the BL at Baltimore originated at altitudes of several kilometers. In other cases, back trajectories can end up at ground level, in which case their tracks may be considered unreliable.

Here, we focus on results obtained with trajectory ensembles initialized at 500m, as representative of the atmospheric mixed layer, which grows to a thickness of typically 1.5 km in summer afternoons. The use of trajectory *clusters* permits dispersion during transport due to small initial horizontal displacements; even with initial displacements that are much smaller than the resolution of the MCIP winds, trajectories can ultimately separate due to the chaotic nature of synoptic-scale atmospheric flows (Pierce and Fairlie, 1993). Trajectory clusters that remain coherent over the duration of the transport provide greater confidence that Lagrangian-mean characteristics are representative. In most cases we have found that trajectory clusters remain coherent up to 3 days. On the other hand, they can disperse very rapidly on encounters with latent heat or stagnation points in the flow.

2.4 Methods for source attribution

An important objective of this study is to characterize the origin of fine particulate and sulfate pollution at the receptor site, Baltimore, and to estimate the relative contributions of local emissions and regional transport for the most polluted days at the recptor site. For this purpose we define a local domain around Baltimore - a circle with a radius of 80 km, centered at 39.3^{o}N, 76.6^{o}W, which includes the northern Chesapeake Bay, Washington, DC, and a small part of southern Pennsylvania. The domain is shown in Fig.2**.** We refer to the region outside the circle as the regional domain.

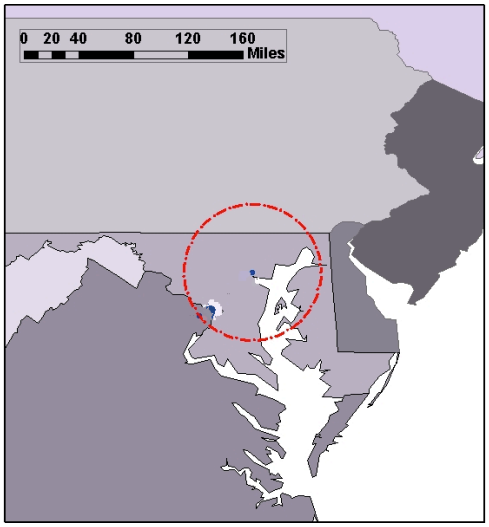

Figure 2: Boundary of 80 km local domain around Baltimore (red dashed circle).

Trajectory ensembles, initialized at the receptor site, are used to track the origin of polluted air masses and estimate the chemical and physical transformations for the 20% most and least polluted days at Baltimore. Source apportionment maps for these groups of days

highlight those source regions upon which air quality at Baltimore largely depends. In addition, Lagrangian-mean changes within and outside the boundary of the Baltimore local domain are used to contrast regional and local influences. These methods are illustrated in Section 4.

3. Observations, CMAQ model results, and an example of Lagrangian sampling

3.1 Overview of air quality in Summer 2004

Summer 2004 was slightly cooler and wetter than average along the United States eastern seaboard and these conditions likely impacted air quality in the Baltimore, MD area (Thompson et al., 2007). The Baltimore region was approximately 1-2 deg F cooler and received about 3-5 more inches of rain, than the 1971-2000 long-term average (Weber et al., 2008). Piety (2004) report significantly fewer days above 90 deg F at Baltimore-Washington Airport (BWI) during June-August 2004, compared with a typical summer (8 days vs. 20 days). Poor air quality in the Mid-Atlantic region is normally associated with hot, dry conditions. Piety (2004) report mean ozone levels lower than normal, in the Baltimore/Washington, DC corridor during Summer 2004, compared with typical values from the period 1990-2003, and only one case for which ozone exceeding the EPA 8-hr standard of 80 ppb.

$PM_{2.5}$ levels are less easy to characterize for summer 2004, compared to normal, because ambient-level particulate concentrations were not measured on an hourly basis consistently prior to 2003. Elevated $PM_{2.5}$ concentrations in Mid-Atlantic, and Northeastern states during summer are often associated with westerly transport of sulfate precursors from the Ohio River Valley region [Dutkiewicz et al., 2004; Hennigan et al., 2006]. However, summer 2004 was characterized by an atypical series of cut-off upper-level low-pressure systems, which impeded westerly transport. On the other hand, PM2.5 formation is favored by the moist conditions in summer 2004, and the eastern seaboard was impacted by organic aerosol from extensive Alaskan wildfires (Clarke et al., 2007; Redemann et al., 2007). Based on the 5 years (2003-2007) of continuous data available, summer 2004 appears to have been characterized by PM2.5 levels typical or slightly worse than normal.

3.2 Evaluation of CMAQ with Observations

Figure 3 shows a time series of observed and simulated $PM_{2.5}$ and sulfate concentrations for summer 2004 for the Baltimore area. Solid lines show observed (black) and simulated (red) $PM_{2.5}$. The observed data are daily averages of 1-hr observations from the TEOM monitor at Old Town, Baltimore. The simulated data are daily averages of CMAQ surface concentrations at Baltimore. Observed sulfate data are taken from STN monitors at Fort Meade, MD, (dark blue), Essex, MD (pale blue), and from the Baltimore IMPROVE site (green squares). Simulated sulfate is shown by the red dotted line. The observations show daily average $PM_{2.5}$ greater than 35 μg m^{-3} on 11, 21, and 22 July, and 24 August. Simulated $PM_{2.5}$ is correlated with the observations (r^2 = 0.7) but underestimates observations (mean bias of -4.4 μg m^{-3}; rms difference of 5.3 μg m^{-3}). Simulated sulfate is also correlated with observations at the EPA surface monitors (r^2 = 0.6) and with observations at the Baltimore IMPROVE site (r^2 = 0.9), though it tends to overestimate observations; mean biases of 1.6 and 0.8 μg m^{-3}, and rms differences of 3.1 and 2.1 μg m^{-3}, compared with STN surface sites, and the Baltimore IMPROVE monitor, respectively. These comparisons indicate that day-to-day variability in surface $PM_{2.5}$ and sulfate is well represented by the model at the Baltimore site, but that the model generally under-predicts surface $PM_{2.5}$ and over-predicts sulfate. Sulfate constitutes a higher fraction of $PM_{2.5}$ in the model compared with surface observations.

The dark blue horizontal lines in Figure 3 at approximately 30.5 and 12.5 μg m^{-3} distinguish the top 20% (dirtiest) and bottom 20% (cleanest) days at the Old Town site, as determined by the daily mean $PM_{2.5}$ concentrations. Of the 18 (of 89) top 20% $PM_{2.5}$ days observed at the Old Town monitor, 12 days (8, 9, 25 June; 2, 11, 20, 21, and 22 July; 10, 11, 24, and 25 August) are also top 20% $PM_{2.5}$ days in the CMAQ simulation, a 67% success rate by this measure. Lagrangian characteristics of the 20% dirtiest and cleanest days are presented and fully discussed in Section 4. The results shown in Figure 3 indicate that despite a low bias for $PM_{2.5}$,, CMAQ shows considerable skill in reproducing the day-to-day variability of fine aerosol at the ground.

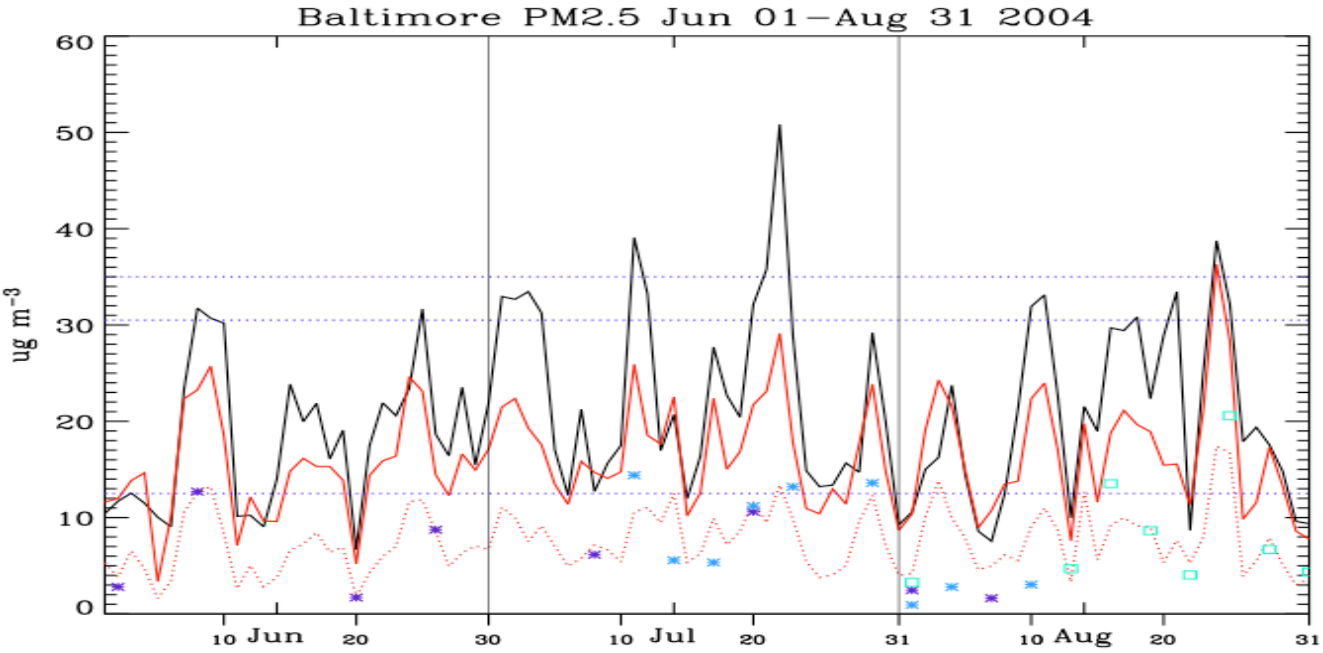

Figure 3. Time series of daily average $PM_{2.5}$ from Old Town Baltimore (black solid line) and from CMAQ (red solid line) for summer 2004. Simulated sulfate (red dotted line) and observed sulfate at Fort Meade, MD, (dark blue star), Essex, MD (pale blue star), and the Baltimore IMPROVE site (green square) are also shown.

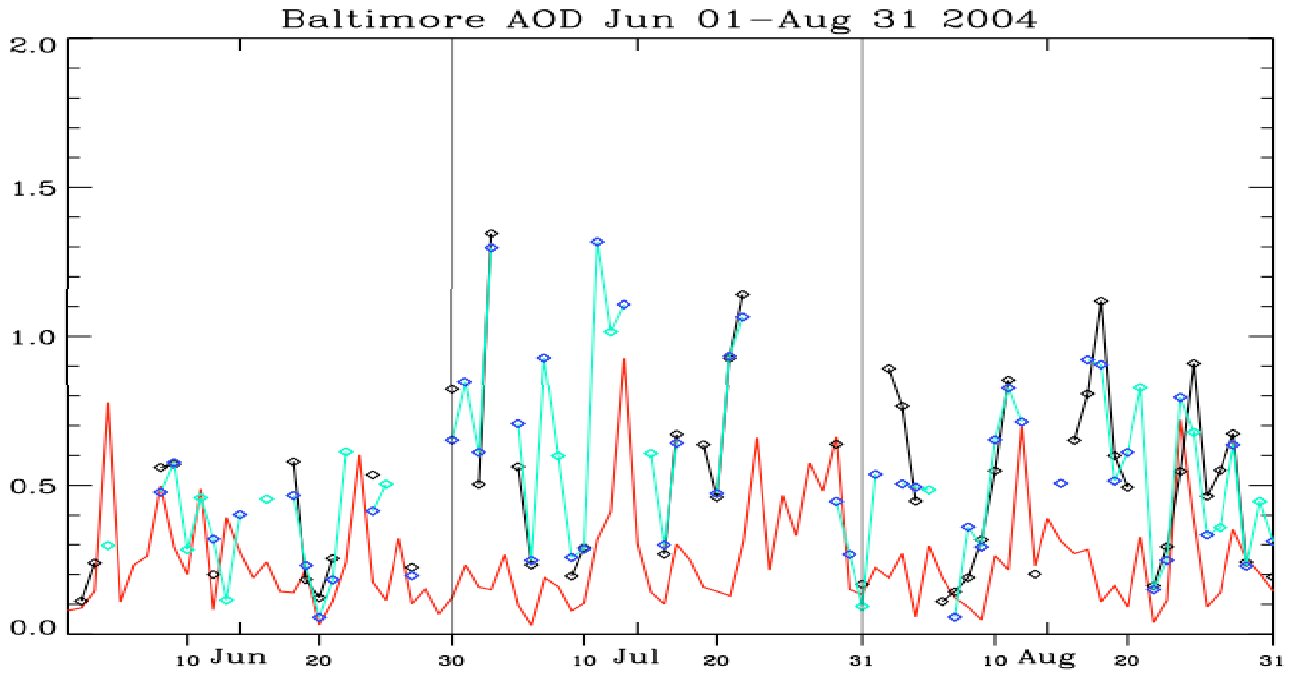

Figure 4: Time series of AOD from the AERONET monitor at Maryland Science Center (black line and diamonds), MODIS (green line, green diamonds for Aqua, blue diamonds for Terra), and from CMAQ (red line) for summer 2004. The MODIS observations are those closest to Baltimore with a 40 km radius, for each day. AERONET and CMAQ results are 15-20Z averages on each day.

Figure 4 shows time series of CMAQ AOD at Baltimore, together with 550 nm AOD obtained from MODIS Aqua and Terra instruments, and estimated 550 nm AOD from the AERONET (ground-based AOD) instrument at the Maryland Science Center. The MODIS observations are those closest to Baltimore within a 40 km radius on each day. The AERONET AOD is estimated from measurements at 500 and 670 nm using the Angstrom exponent relationship for these wavelengths, The CMAQ AOD time series is obtained by vertically integrating profiles of reconstructed aerosol extinction (Equ.1). Both the simulated and AERONET data shown are daily 15 - 18Z averages, spanning the range of times for MODIS overpass at this location. The MODIS and AERONET observations are highly correlated (r^2 = 0.85). CMAQ is positively correlated with both AERONET and MODIS observations, but the percent variance explained is low (12% in each case) with a negative bias of around 0.3, compared with MODIS, and 0.2 compared with the AERONET data. Roy *et al.* (2007) found that monthly mean AOD estimates from CMAQ based on reconstructed extinction taken from a simulation of summer 2001 were on average 0.2 lower than corresponding MODIS AOD observations. Results from Fig. 4 indicate that CMAQ does less well in representing the day-to-day variability in tropospheric fine aerosol columns at Baltimore during summer 2004 than is the case for $PM_{2.5}$ at the surface. Long range transport of pollutants, not represented in this CMAQ simulation, e.g. smoke from Alaskan wildfires in July and August 2004 (Pierce et al. 2007; Pfister et al., 2007; Clarke et al., 2007) most likely contributes to this discrepancy. Limitations in applying the empirical formulation for reconstructed aerosol extinction (Equ. 1) may also contribute to this deficiency.

3.3 The High PM2.5 event of 24 August, 2004: observations, CMAQ results, and trajectory sampling.

Here we look specifically at the high PM2.5 event of 24 August, 2004. Figure 5 shows an NCEP surface analysis at 11Z on 24 August, and a map of CMAQ surface PM2.5, with AirNOW PM2.5 observations for the same time. CMAQ shows a band of high aerosols stretching from the Midwest to offshore in the Atlantic, associated with a weak frontal system. Surface observations from the AirNOW TEOM network of monitors show qualitatively good agreement with the simulated aerosol pattern.

Figure 6 shows corresponding maps of MODIS (Terra) AOD and COT for 24 August, together with CMAQ reconstructed AOD for the same day. MODIS shows high AOD and COT over much of the Mid-Atlantic region. High optical depth over much of PA, MI, eastern KY and TN, and western NC and SC, and offshore is characterized as cloud, rather than aerosol, by MODIS. CMAQ AOD shows a similar spatial distribution to the surface PM2.5 pattern (Fig. 5) and good qualitative agreement with distribution of AOD and COT shown by MODIS.

Figure 7 shows 3-day ensemble back trajectories initialized at Baltimore at 18Z, on Aug. 24. The trajectory ensembles are color coded according to their initial altitudes: 20m (dark blue), 100m (pale blue); 500m (green); 1000m (red). Colored circles show principal SO_2 surface emissions. The trajectory ensembles are shown to originate to the west, passing through OH, PA, WV and MD, characterized by multiple surface SO_2 sources.

Figure 8 shows shows time series of altitude, and SO_2, sulfate, relative humidity, $PM_{2.5}$, and aerosol extinction sampled from the CMAQ model along the back trajectories shown in Fig.7 (we refer to these as Lagrangian time series). The trajectories are color coded as in Fig. 7. Solid lines show the cluster mean values, while separate points show values for individual trajectories. Crosses (also color-coded) mark the boundary layer (BL) height when trajectories encounter the BL, and are reproduced across all panels, with an altitude scale to the right of each panel. These time series give a Lagrangian perspective of some key chemical and physical histories of air contributing to BL composition over Baltimore on 24 August. The top left panel shows that most trajectory ensembles descend from around 2 km over the course of 3-day transport, and encounter the daytime BL on each of the 3 days. The trajectories encounter elevated SO_2, sulfate, and PM2.5 in the daytime BL, particularly 48 hours upstream of Baltimore. This is particularly striking for trajectories initialized at 1000m, which pass through eastern OH and PA. Peak sulfate of sulfate of around 15 $\mu g\ m^{-3}$ (PM2.5 around 30 $\mu g\ m^{-3}$) are attained over the Baltimore site. (The remainder of

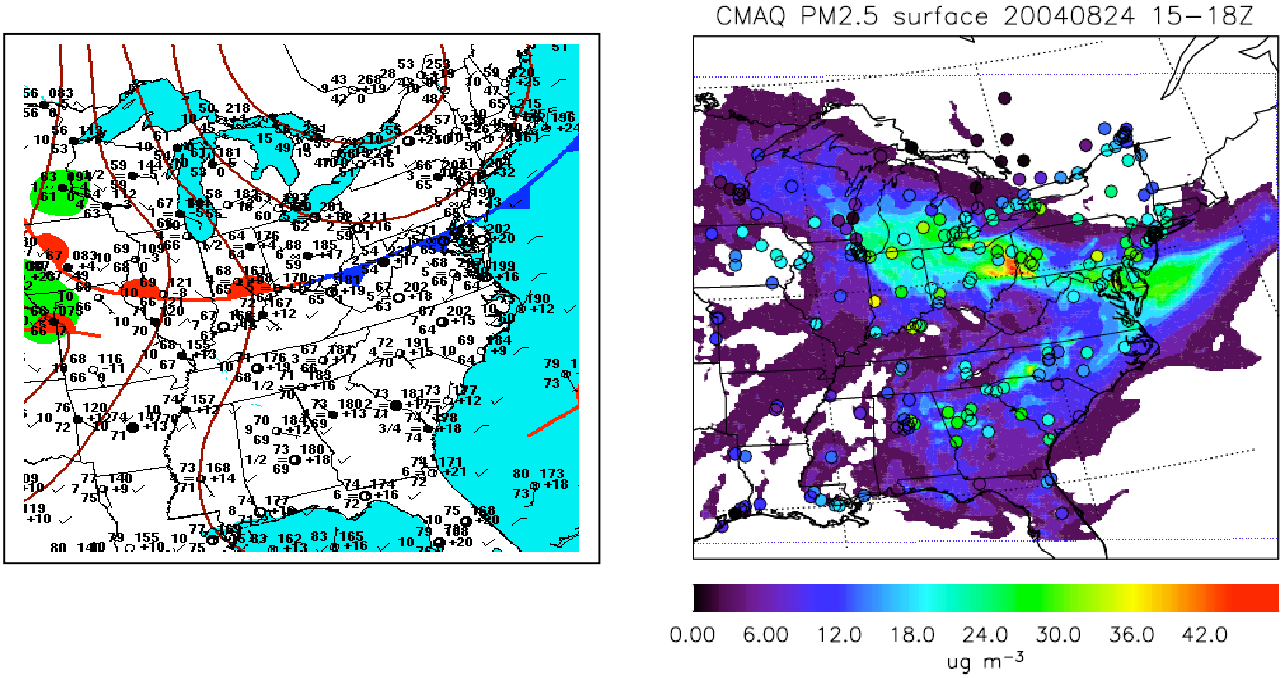

Figure 5. NCEP surface analysis 11Z, (left), and CMAQ surface and AirNOW (TEOM) PM2.5, 15-18Z (right), 24 August, 2004.

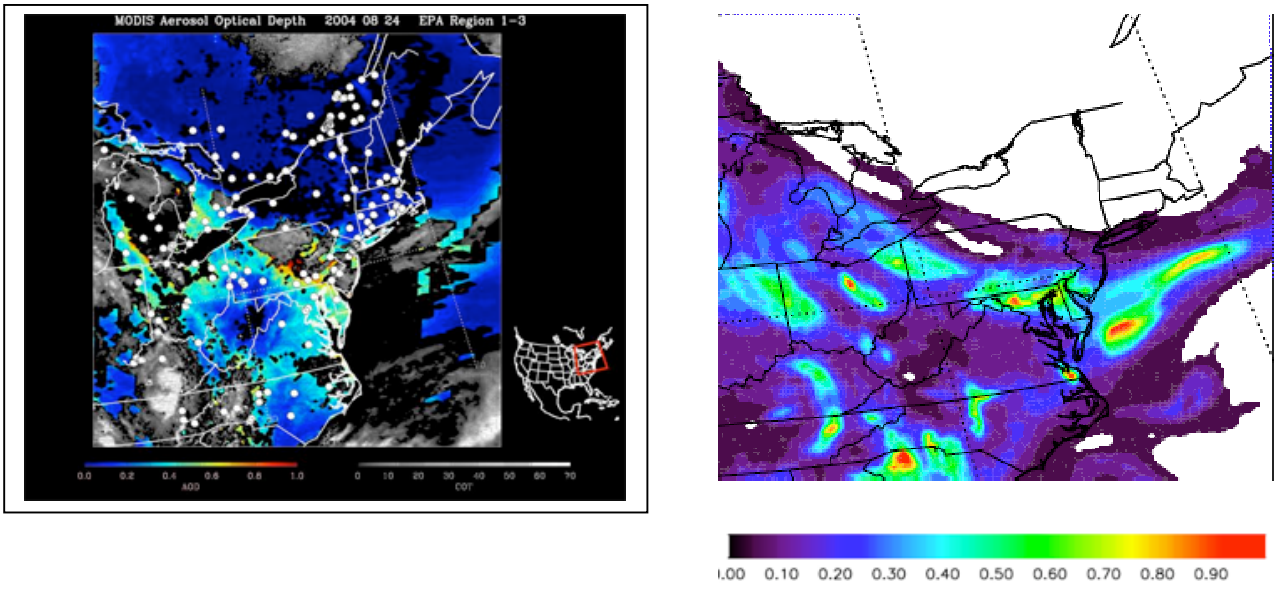

Figure 6. MODIS (Terra) AOD and COT (left), and CMAQ reconstructed AOD (right), 15-18Z, 24 August, 2004.

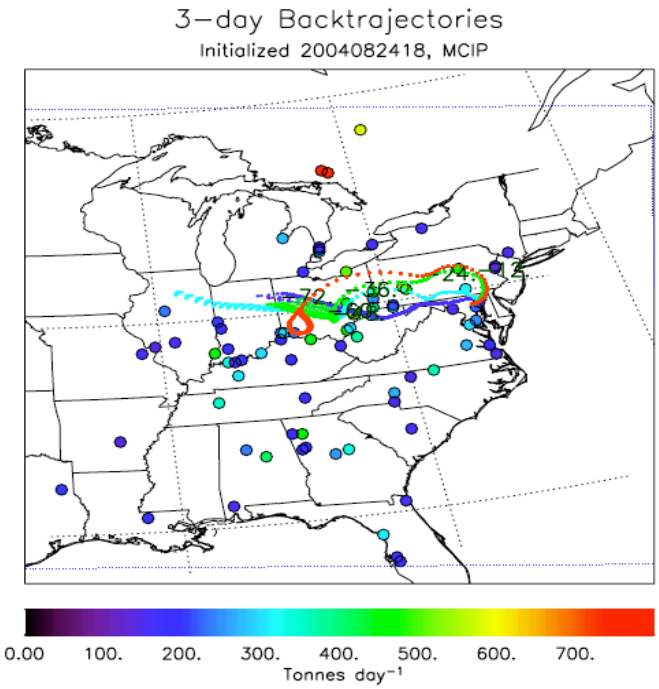

Figure 7. 3-day Ensemble back trajectories initialized at Baltimore at 18Z, Aug. 24. Initial trajectory altitudes: 20m (dark blue), 100m (pale blue); 500m (green); 1000m (red). Time stamps (hrs) mark 500m trajectories. Colored circles show principal SO_2 surface emissions.

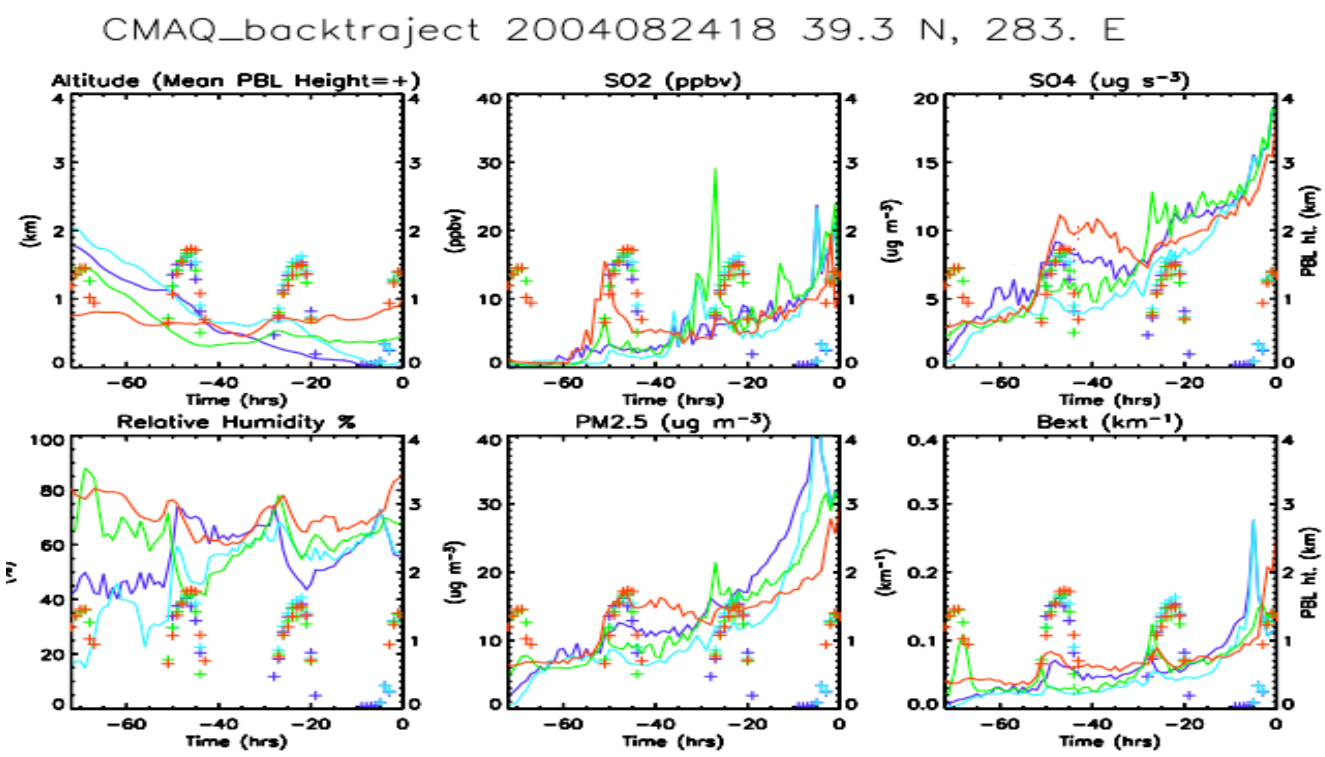

Figure 8. Lagrangian timeseries for trajectories initialized at Baltimore at 18Z, Aug. 24. Color coding as for Fig. 7. Color-coded crosses show BL height for trajectories that are in the BL.

PM2.5 is largely taken up by organic aerosol, not shown). Reconstructed aerosol extinction, which closely tracks relative humidity, reaches up to 0.2 km^{-1} in the lowest 1 km at Baltimore.

Figure 9 shows Lagrangian curtains of SO_2 emissions, SO_2, sulfate, relative humidity, $PM_{2.5}$, and aerosol extinction for the trajectory ensemble initialized at 500m at 18Z on 24 August. Lagrangian curtains are time series of ensemble-mean vertical profiles sampled from the CMAQ fields, and provide an additional (vertical) dimension to the information shown in the Lagrangian time series (Fig. 8). The trajectory ensemble initialized at 500m provides a sample of the air that contributes to the BL at Baltimore on 24 August. The solid black line shows the ensemble-mean altitude for these trajectories. Vertical lines in each panel show the distance of the ensemble-mean location from Baltimore, in 80 km intervals; in this case, the ensemble-mean crosses the boundary of the 80-km local domain approximately 7 hours before reaching Baltimore. Figure 9 shows the vertical extent of elevated SO_2, and sulfate encountered by the trajectory ensemble, particularly around 48, 15 and 5 hours upstream of Baltimore. The figure shows that highest sulfate (around 15 µg m-3) and PM2.5 (around 30 µg m-3) are attained inside the local domain around Baltimore.

4. Ensemble-mean trajectory characteristics and source apportionment for most and least most polluted days

4.1 Ensemble-mean trajectory characteristics

Figure 10 shows time series of key ensemble-mean CMAQ chemical and physical characteristics for trajectory ensembles initialized at 500 m for summer 2004: (i) distance from Baltimore, (ii) altitude, (iii) SO_2, (iv) sulfate,(v) $PM_{2.5}$, and (vi) rain. Timeseries are shown for each of the 89 daily trajectory simulations initialized at 18Z conducted over the summer (4 June – 31 August); Red stars to the right of each panel mark the top 20% observed PM2.5 days at Baltimore; the bottom 20% (cleanest) days are marked with the blue stars. Ensemble-mean trajectory characteristics at Baltimore are found at 0 h on the right side of each panel, while conditions 3 days upstream (-72 h) are found on the left side of each panel. The solid red line in each panel indicates the times at which the trajectory ensemble for each simulation intersects the local domain boundary 80 km from Baltimore.

Simulated high sulfate and $PM_{2.5}$ events at Baltimore appear as the warmest colors on the right side of the respective panels. Many of these events coincide with top 20% observed $PM_{2.5}$ days marked by the red stars, notably 8-9, and 25 June, 1-2, 11-12, 20-22 July, 10-11, 18, 24-25 August. These events typically show the following ensemble mean characteristics in the final 48 hours before arriving at Baltimore: (i) the trajectories generally originate from a distance less than 1000 km; (ii) they generally remain below 2 km altitude; (iii) they experience little or no rain; (iv) they experience elevated SO_2 (5 - 30 ppbv), and show a history of elevated sulfate and $PM_{2.5}$. Cleanest days at Baltimore tend to be associated with trajectory ensembles that originate from greater distances, e.g. 11, 20 June, 6, 15 July, and 22 August, and higher elevations, or experience rain during transport. These characteristics are consistent with our understanding that the most polluted days are associated with air that is regularly exposed to boundary layer sources, within a moderate range of Baltimore (0 - 1000 km).

The red contour in Fig. 10 shows intersections with the 80-km local domain boundary around Baltimore. Trajectory ensembles characterized by high sulfate, $PM_{2.5}$ and/or SO_2 outside the boundary of the local domain demonstrate that regional transport impacts sulfate and $PM_{2.5}$ concentrations at Baltimore. For the case of 24-25 August, for example, the trajectory cluster arrives at the boundary 7 hours or so before reaching Baltimore, with sulfate already elevated beyond 12 µg m^{-3}. Nonetheless, in this case, an increase in sulfate of more than 30% occurs within the local domain around Baltimore. For the case of 11 July, on the other hand, most of the increase in sulfate occurs within 80km of Baltimore. In addition, the boundary contour highlights cases of recirculation, when multiple intersections with the local domain boundary occur. Several examples of recirculation are evident for trajectory ensembles initialized at 500 m. Examples include 7 June, when the local domain boundary is encountered 40 hours before arrival, 21 June, 7, 12, and 14 July, 13, and 16 August. Figure 10 gives no indication that recirculation affects the top 20% polluted days.

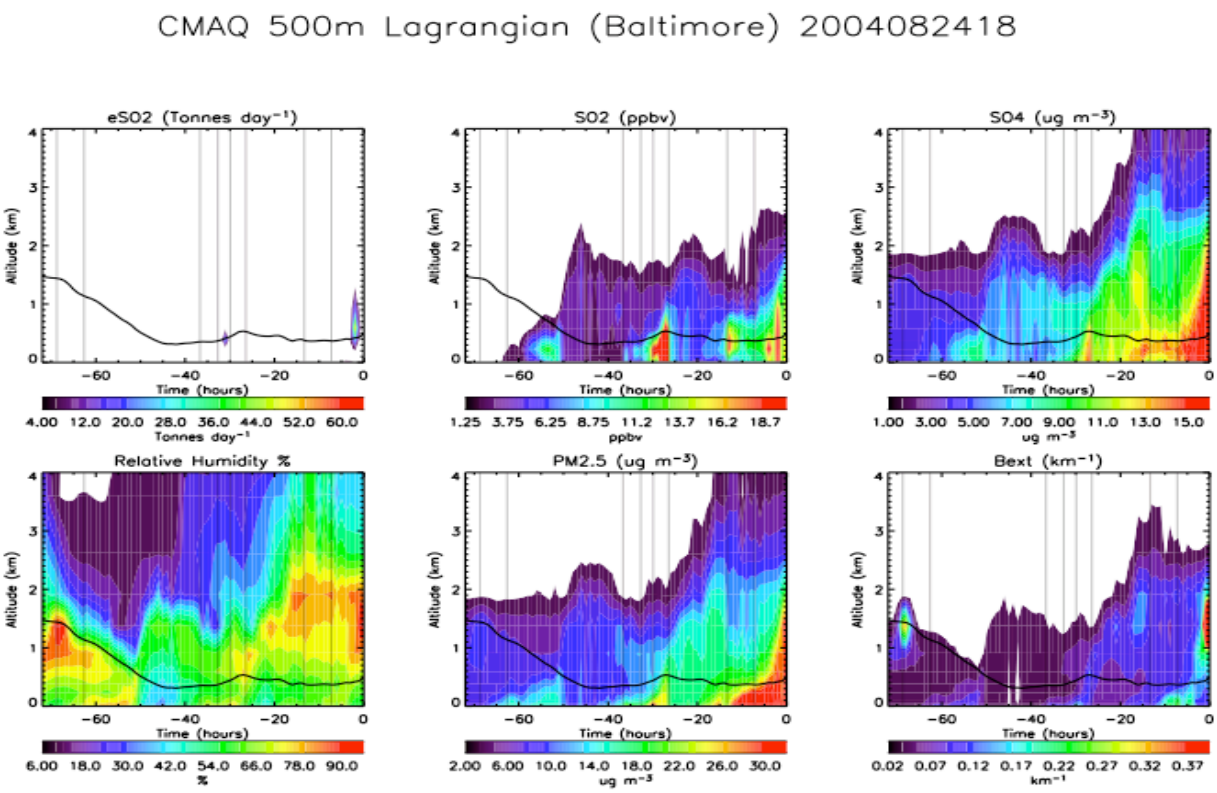

Figure 9. 3-day Lagrangian curtains for trajectories initialized at 500m at Baltimore at 18Z, 24 August, 2004.

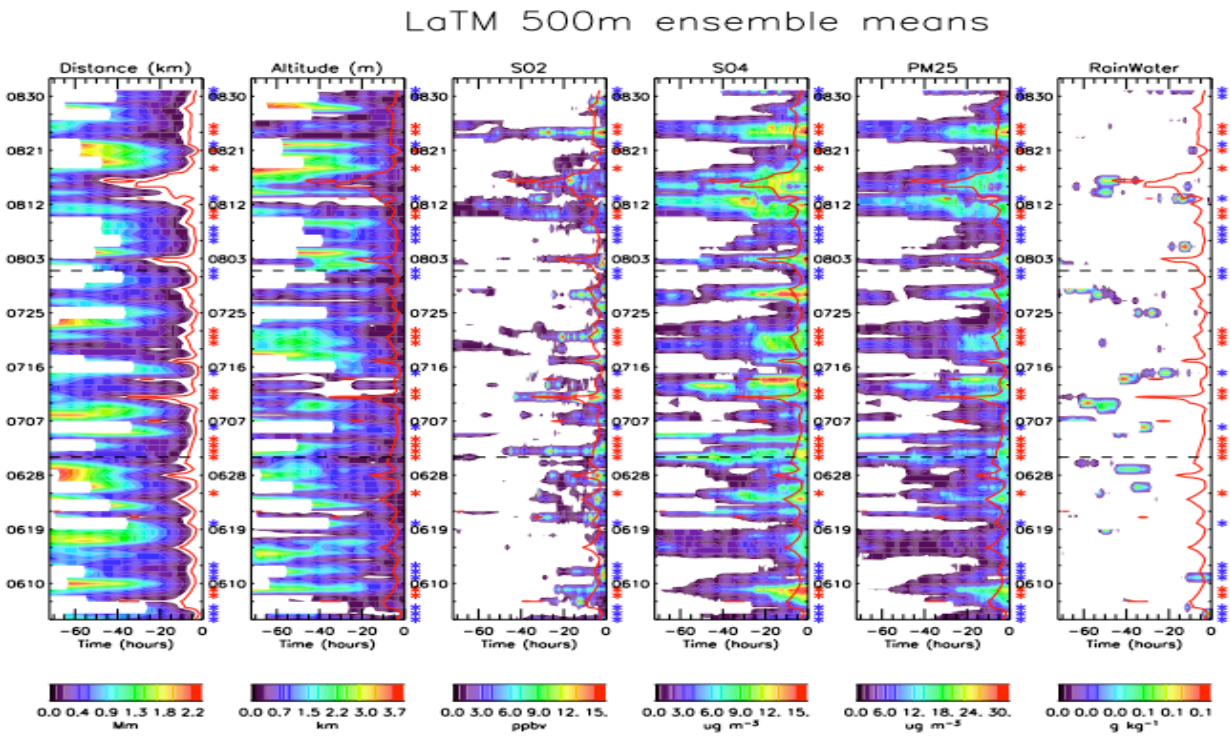

Figure 10. Time series of trajectory ensemble-mean characteristics for trajectory simulations conducted from 4 June to 31 August. Trajectories are initialized at Baltimore at 500m at 18Z each day..

4.2 Measures of regional vs. local contributions

An important goal is to estimate the relative impact of local and regional transport contributions to fine particulate and sulfate concentrations at the receptor site, Baltimore. We have computed ensemble-mean changes in sulfate, PM2.5, and SO_2, inside and outside the local domain, for each of the daily trajectory simulations. These measures are attributed to regional transport and local impacts respectively. (Note that in the case of recirculation, multiple time periods can contribute to these measures.)

Figure 11 shows ensemble-mean changes in sulfate for the 89 trajectory simulations conducted for the summer (4 June – 31 August). The black bars show the total ensemble-mean change over 3 days, while the overlaid red bars show ensemble-mean change that occurs outside the 80-km local domain. The difference in length between the black and red bars represents the ensemble-mean change that occurs in the local domain, and is sometimes negative. Asterisks above the bars mark the top 20% (red) and bottom 20% (navy) observed PM2.5 days at Baltimore. Table 1 presents these measures for sulfate and PM2.5 for the top 20% (dirtiest) days observed at Baltimore. Also shown in the table for each constituent is the percentage, X, of the total change that occurs outside the local domain, attributed to region transport. We consider values of $X > 65\%$ to indicate predominantly regional influence; $X < 35\%$ to indicate predominantly local influence; and $35 < X < 65\%$ as combined or mixed influence.

Table 1 indicates that for the 20% most polluted days at Baltimore, regional transport makes the largest contribution to sulfate and PM2.5 at Baltimore. On 24 August, for example, almost 80% of the change in PM2.5 is attributed to regional transport. Of the 18 top 20% days, only 3 (3 June, 11 June, and 25 August) show larger local vs. regional contributions for sulfate and PM2.5. In some cases the ensemble-mean change in the local domain is negative, e.g. for 20-22 July, corresponding to losses due to moist processes or diffusive mixing.

4.3 Transport patterns and source attribution maps

Figure 12 shows maps of spatially averaged trajectory characteristics for the top 20% $PM_{2.5}$ days observed at Baltimore (again we select trajectory ensembles initialized at 500m). These maps are constructed by averaging over the whole summer the chemical and physical characteristics of all trajectories passing through grid-squares of approximately 50 by 50 km. Shown are (i) the trajectory counts, (ii) SO_2 emissions (iii) SO_2 mixing ratio (ppbv), (iv) sulfate concentration (μg m^{-3}), (v) altitude (km), and (vi) $PM_{2.5}$ concentration (μg m^{-3}). The map of trajectory counts forms a relatively compact crescent shape, with highest count densities extending from eastern NC, through VA, MD and southern PA, WV into OH, where branches to TN and MI are found. This crescent shape reflects principal transport routes from the OH valley through PA, and from southeast VA, and eastern NC. Panel (ii) highlights encounters with SO_2 sources up to 15 Tonnes day^{-1} in the Ohio Valley, and PA. Panel (iii) shows peak SO_2 values in western and southern PA and MD. Panels (iv) and (vi) show the principal transport pathways associated with highest sulfate and $PM_{2.5}$ concentrations. Panel (v) shows that trajectories associated with the most polluted days at Baltimore can originate at altitudes up to 4 km, 3 days upstream, but more typically descend from altitudes of 2 km or less in their approach into Baltimore, consistent with the findings of Fig. 10.

Figure 13 shows corresponding maps of spatially averaged trajectory characteristics for the 20% least polluted $PM_{2.5}$ days observed at Baltimore. The map of trajectory counts is very different from that in Fig. 12 for the top 20% days. Principal transport routes for clean days include trajectory paths from points north and northwest, including Ontario, and from offshore. In particular, none of the air parcel ensembles originates in the OH Valley and points further west and south. Despite encountering some SO_2 sources over PA, spatially averaged SO_2 and sulfate values do not rise above 7 ppm and 8 μg m^{-3} respectively.

5. Conclusions

This study uses ensemble-mean Lagrangian sampling of CMAQ model fields to characterize chemical and physical histories of air that contributes to sulfate and PM2.5 concentrations in the afternoon BL at Baltimore in summer 2004. We estimate “regional tranport” and

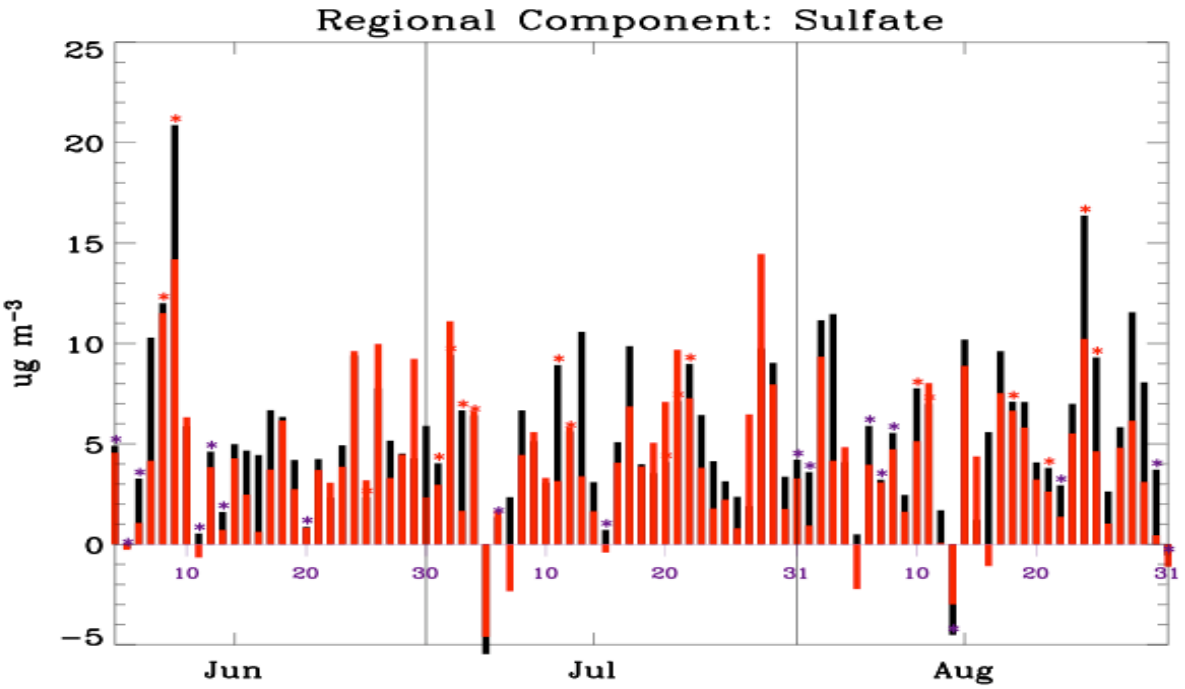

Figure 11. Regional (red) vs. Total (black) ensemble-mean changes in sulfate for trajectory simulations conducted from 4 June to 31 August. Trajectories are initialized at Baltimore at 500m**.** Red stars mark top 20% observed PM2.5 days at Baltimore; blue stars mark bottom 20%.

500m trajectories: Ensemble-mean changes in Sulfate and PM2.5								
	Delta PM2.5				Delta Sulfate			
date	Local	Regional	Total	X(%)	Local	Regional	Total	X(%)
0608	2.58	14.45	17.02	84.87	0.51	11.51	12.01	95.77
0609	8.75	17.74	26.49	66.98	6.69	14.20	20.88	67.97
0625	-1.06	6.20	5.14	>100%	-0.84	3.19	2.34	>100%
0701	0.99	2.24	3.23	69.45	1.07	2.96	4.04	73.45
0702	-0.12	16.03	15.92	>100%	-1.69	11.11	9.43	>100%
0703	9.12	3.32	12.44	26.66	5.00	1.66	6.67	24.97
0704	0.62	7.49	8.10	92.40	-0.22	6.64	6.42	>100%
0711	9.71	6.55	16.26	40.29	5.78	3.15	8.93	35.26
0712	-1.31	7.56	6.25	>100%	-0.23	5.84	5.62	>100%
0720	-1.97	3.35	1.38	>100%	-2.99	7.09	4.10	>100%
0721	-2.49	14.13	11.64	>100%	-2.56	9.69	7.14	>100%
0722	-3.29	16.42	13.13	>100%	1.71	7.27	8.98	80.92
0810	4.98	8.40	13.38	62.77	2.64	5.13	7.77	66.04
0811	-2.85	12.73	9.88	>100%	-1.03	8.03	7.00	>100%
0818	3.08	8.24	11.32	72.78	0.45	6.65	7.10	93.68
0821	1.80	3.13	4.93	63.51	1.20	2.62	3.81	68.62
0824	5.44	19.66	25.10	78.32	6.14	10.23	16.37	62.49
0825	7.45	3.46	10.91	31.71	4.67	4.63	9.31	49.77

Table 1: Regional, local and total Lagrangian mean contributions to PM2.5 and sulfate for the top 20% PM2.5 days observedat Baltimore:. Blue shading marks days with predominant (> 65%) regional contribution, X.

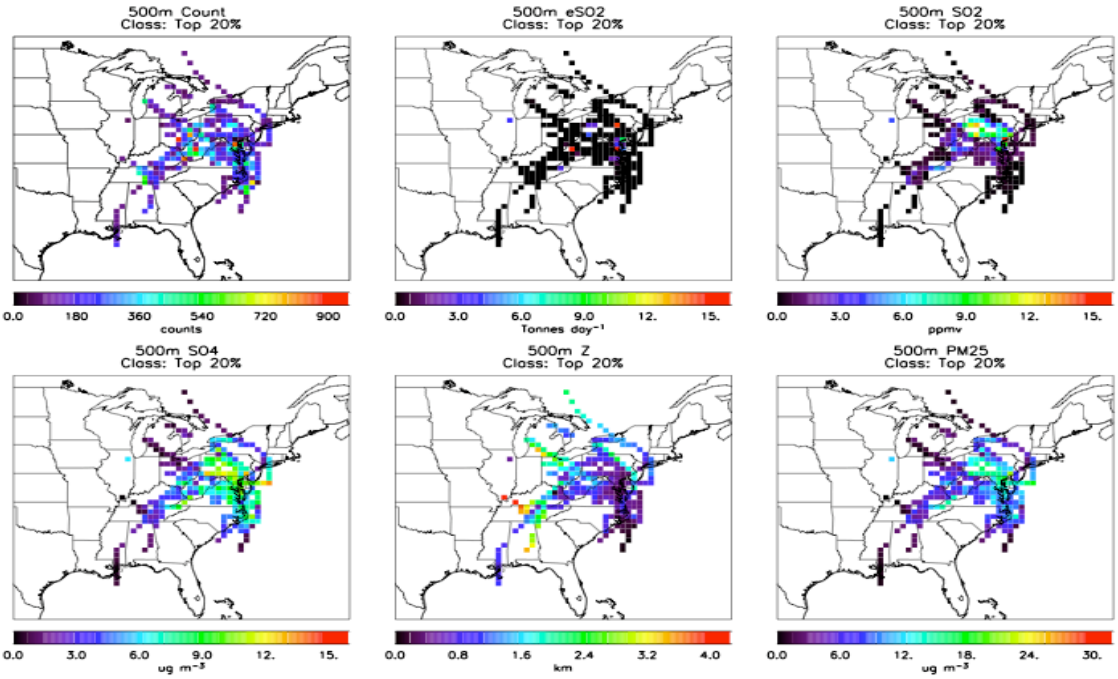

Figure 12: Spatially averaged trajectory characteristics for the top 20% $PM_{2.5}$ days observed at Baltimore (500m trajectories). Shown are (i) the trajectory counts, (ii) SO_2 emissions (iii) SO_2 mixing ratio (ppbv), (iv) sulfate concentration (μg m^{-3}), (v) altitude (km), and (vi) $PM_{2.5}$ concentration (μg m^{-3}).

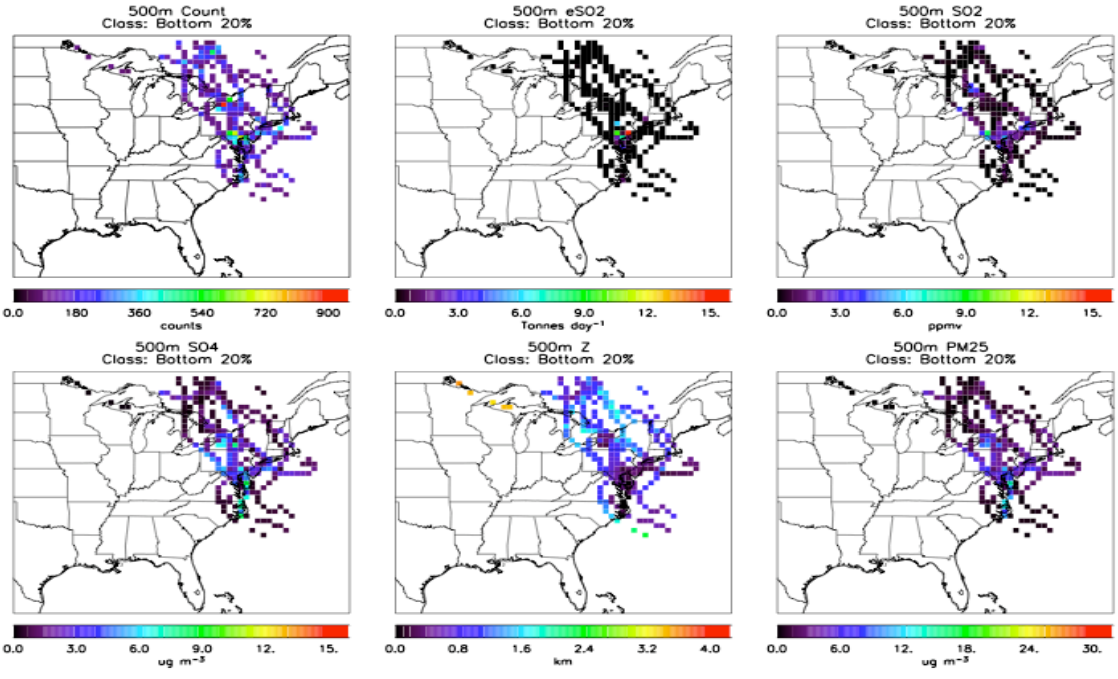

Figure 13: As for Fig. 12, but for the bottom 20% PM2.5 days observed at Baltimore, summer 2004.

"local" contributions by computing ensemble-mean changes inside and outside an 80-km-radius local domain around Baltimore. Results indicate that a large majority of the top 20% observed (most polluted) PM2.5 days at Baltimore are predominantly impacted by regional transport of PM2.5 (primarily sulfate). The results provide support for the OH Valley air-shed as being a principal upstream source region for PM2.5 pollution at Baltimore. Thus, reductions in SO_2 emissions from that region, implemented under CAIR, may be expected to significantly impact particulate air quality in Baltimore.

The study serves as a prototype that may be useful for city, state and regional air quality agencies as they evaluate sources of air pollution in their areas, determine how to reduce ambient fine particle concentrations from local and regional sources, and reduce the impact of particulate pollution downwind. While Baltimore is the focus here, the techniques may be applied to multiple locations across the eastern U.S**.** The NASA LaRC trajectory model and analysis software have been transitioned to the EPA's Remote Sensing Information Gateway (RSIG), which feeds the AirQuest system, a database that merges Three-dimensional Air Quality System (3D-AQS) and AIRNow data for the continental U.S. with other observed, modeled, and socioeconomic data. By having the 3D-AQS data made available via RSIG and AirQuest, analysis tools can be automated and results made available to multiple users on request.

A number of improvements are needed to fully exploit trajectory sampling of CMAQ model results in future applications. First, the CMAQ simulation used here employs clean lateral boundary conditions. Although sulfate precursor sources external to the CMAQ domain may not be important to capture an adequate simulation of sulfate at east coast sites, observations clearly indicate that such an approach does not work for PM2.5 as a whole. Particulate pollution from wild fires in Canada and Alaska made a significant contribution to air quality along the eastern seaboard during summer 2004 (Pfister et al., 2005; Pierce et al., 2007; Clarke et al., 2007). Future applications would benefit from boundary conditions provided from a larger domain simulation complete with time-dependent wildfire sources based on observations. Moreover, monitoring the impact of CAIR reductions in anthropogenic emissions will require emission inventories that keep pace with current conditions. In addition, the CMAQ simulation used for this study did not archive 3-d fields of chemical and physical tendencies for sulfate and sulfate precursors, e.g. 3-d chemical production and loss, and convective mixing tendencies. Such fields are necessary to estimate separately chemical and physical tendencies along back trajectories, and to close the sulfate budget.

Acknowlegements:

We wish to thank Tanya Otte and colleagues at Research Triangle Park for providing the CMAQ model and MCIP meteorological fields used in this study. We thank the NASA MODIS team for the use of their data. We thank the AERONET and IMPROVE science teams for online provision of their data. Thanks to the Maryland Department of Environment and to MARAMA for reviews on this work. Special thanks to Ray Hoff of UMBC and Dev Roy of EPA for their technical input and discussions.

References:

Binkowski, F.S., and S.J. Roselle. (2003). " Models-3 Community Multiscale Air Quality (CMAQ) model aerosol component, 1. Model Description." *Journal of Geophysical Research*, 108, D6, 4183, doi:10.1029/2001JD001409.

Byun, D.W., and J.K.S. Ching. (1999). "Science Algorithms of the EPA Models-3 Community Multiscale Air Quality (CMAQ) Modeling System." U.S. Environmental Protection Agency, EPA/600/R-99/030.

Byun, D.W., and K.L. Schere. (2006). "Review of the governing equations, computational algorithms, and other components of the Models-3 Community Multiscale Air Quality (CMAQ) Modeling system." *Applied Mechanics Reviews*, 59, 51-77.

Clarke, A., et al. (2007), Biomass burning and pollution aerosol over North America: Organic components and their influence on spectral optical properties and humidification response, *J. Geophys. Res*., 112, D12S18, doi:10.1029/2006JD007777.

Dutkiewicz, V. A., S. Qureshi, A. R. Khan, V. Ferraro, J. Schwab, K. Demerjian, and L. Husain (2004), Sources of fine particulate sulfate in New York, *Atmos. Environ*., 38(20), 3179– 3189.

Fast, J. D., Rahul A. Zaveri, Xindi Bian, Elaine G. Chapman, and Richard C. Easter, Effect of regional-scale transport on oxidants in the vicinity of Philadelphia during the 1999 NE-OPS field campaign, *J. Geophys. Res*., 107(D16), 4307,

10.1029/2001JD000980, 2002.
Gery, M. W., G. Z. Whitten, J. P. Killus, and M. C. Dodge (1989). “A photochemical kinetics mechanism for urban and regional scale computer modeling.” *Journal of Geophysical Research*, 94, 12,925–12,956.
Hennigan, C. J., S. Sandholm, S. Kim, R. E. Stickel, L. G. Huey, and R. J. Weber (2006), Influence of Ohio River valley emissions on fine particle sulfate measured from aircraft over large regions of the eastern United States and Canada during INTEX-NA*, J. Geophys. Res*., 111, D24S04, doi:10.1029/2006JD007282.
Malm, W.C., et al. (1994). “Spatial and seasonal trends in particle concentration and opticalextinction in the United States.” *Journal of Geophysical Research,* Vol. 99, No D1, 1347-1370.
Nenes, A., Pilinis, C., Pandis, S.N. (1998). “ISORROPIA: A New Thermodynamic Model for Multiphase Multicomponent Inorganic Aerosols.” *Aquat. Geochem*., 4, 123-152.
Pfister, G., P. G. Hess, L. K. Emmons, J.-F. Lamarque, C. Wiedinmyer, D. P. Edwards, G. Pe´tron, J. C. Gille, and G. W. Sachse (2005), Quantifying CO emissions from the 2004 Alaskan wildfires using MOPITT CO data, *Geophys. Res. Lett.*, 32, L11809, doi:10.1029/2005GL022995.
Pierce, R.B., and Fairlie, T.D. (1993). “Chaotic advection in the stratosphere: Implications for the dispersal of chemically perturbed air from the polar vortex.” *Journal of Geophysical Research*, 98(D10), pp 18589-18595.
Pierce, R.B., Fairlie, T. D., Grose, W. L., Swinbank, R., and O’Neill, A. (1994). “Mixing Processes within the Polar Night Jet.” *J. Atmos. Sci.*, Vol. 51, No. 20, pp. 2957-2972.
Pierce, R. B., et al. (2007), Chemical data assimilation estimates of continental U.S. ozone and nitrogen budgets during the Intercontinental Chemical Transport Experiment–North America, J. Geophys. Res., 112, D12S21, doi:10.1029/2006JD007722.
Piety, Charles A. (2004). “Air Quality Forecasts for the Metropolitan Baltimore Area – 2004 Final Report.” Submitted to the Maryland Department of the Environment, December 16, 2004.
Redemann, J., et al. (2006), Airborne measurements of spectral direct aerosol radiative forcing in the Intercontinental chemical Transport Experiment/ Intercontinental Transport and Chemical Transformation of anthropogenic pollution, 2004, *J. Geophys. Res*., 111, D14210, doi:10.1029/2005JD006812.
Roy, B. R. Mahur, A.B. Gilliland, and S.C. Howard, A comparison of CMAQ-based aerosol properties with IMPROVE, MODIS, and AERONET data, *J. Geophys. Res*. 112, D14301, doi:10.1029/2006JD008085.
Stohl, A., M. Hittenberger, and G. Wotawa (1998): Validation of the Lagrangian particle dispersion model FLEXPART against large scale tracer experiments. *Atmos. Environ*. 32, 4245-4264.
Tao, Z., S. M. Larson, D. J. Wuebbles, A. Williams, and M. Caughey, A summer simulation of biogenic contributions to ground-level ozone over the continental United States, *J. Geophys. Res*., 108(D14), 4404, doi:10.1029/2002JD002945, 2003.
Thompson, A. M., et al. (2007), Intercontinental Chemical Transport Experiment Ozonesonde Network Study (IONS) 2004: 1. Summertime upper troposphere/lower stratosphere ozone over northeastern North America, *J. Geophys. Res.*, 11 2 , D12S12, doi:10.1029/2006JD007441.